IEEE Access
Multidisciplinary ⋮ Rapid Review ⋮ Open Access Journal

Received August 20, 2020, accepted August 26, 2020, date of publication August 31, 2020, date of current version September 11, 2020.

Digital Object Identifier 10.1109/ACCESS.2020.3020571

High Accuracy Profile Measurement With a New Virtual Multi-Probe Scanning System

NING CHAI [1], **ZIQIANG YIN** [1,2], **AND JIANHUA YAO** [1]

[1]State Key Laboratory of Precision Electronic Manufacturing Technology and Equipment, Guangdong University of Technology, Guangzhou 510000, China
[2]Guangdong Provincial Key Laboratory of Micro-Nano Manufacturing Technology and Equipment, Guangdong University of Technology, Guangzhou 510000, China

Corresponding author: Ziqiang Yin (zqyin@gdut.edu.cn)

This work was supported in part by the National Natural Science Foundation of China under Grant 51575520, and in part by the Science and Technology Program of Guangzhou, China, under Grant 201804020040.

ABSTRACT We present a novel virtual multi-probe scanning system and a new error separation method for the exact optical profile reconstruction. The system realized the multi-probe function by a single probe that fixed on a flexible hinge stage. The flexible hinge stage has a millimeter-level travel range and driven by a voice coil motor to realize the function of the multi-probe. In this work, a high accuracy profile measurement with a high lateral resolution is realized under the errors of the straightness, zero-adjustment, and yaw. The new method can obtain multiple sets of straightness error of the guideway in one scanning measurement. This novel virtual multi-probe scanning system and its corresponding method has the following benefits: (i) using a single probe to separate straightness error without reversal, and can accurately reconstruct the profile, (ii) the reconstructed profile has a very high lateral resolution, depending on the lateral resolution (μm level) of the probe, (iii) the cumulative amplification effect of zero-adjustment error can be eliminated by our method, (iv) the new method can obtain multiple sets of straightness error with higher reliability and accuracy compared with only one set. These benefits are proved by theoretical derivation and simulation. Experiments also prove that the new method can reconstruct the profile with high accuracy and lateral resolution.

INDEX TERMS Straightness, flexible hinge, multi-probe, error elimination.

I. INTRODUCTION

The performance of the high-precision optical system composed of multiple spherical optical components is limited by aberration. To overcome this limitation, aspheric and freeform optical components are developed. Geometric aberrations can be effectively decreased or even eliminated. In the meantime, the number of optical components required for the optical system can be reduced, greatly reducing the dimension and weight of the optical system. Although freeform surfaces can achieve high performance, the profile accuracy must be close to submicron or less, which brings challenges to optical manufacturing and measurement. With the continuous development of freeform manufacturing technology, higher accuracy measurement is the key to freeform manufacturing and application.

In the field of optical profile scanning measurement, the straightness of the scanning stage is the main factor affecting the measurement accuracy. The earliest single-probe reversal method was used to eliminate the straightness error of the scanning stage [1]–[3]. Later, to eliminate the straightness error of the scanning stage more accurately and reliably, the multi-probe scanning method is proposed to solve the straightness error separation problem and has been developed from the two-probe method and the three-probe method to the multi-probe method. The two-probe method uses two probes to eliminate the straightness error [4]–[8], the sequential two-probe method (STP), the combined two-probe method (CTP), and the generalized two-probe method (GTP) included. The advantage is that the two-probe method does not contain the zero-adjustment error of the multi-probe and can completely separate the straightness error. However, the yaw error of the scanning stage cannot be eliminated. To eliminate the yaw error three-probe methods are proposed [9], [10], including the sequential three-probe method (STRP), the combined three- probe method (CTRP), and the generalized three-probe method (GTEP). Although the three-probe methods can eliminate the yaw error, the zero-adjustment error between the three probes will introduce a parabolic cumulative term in the profile evaluation result, which is the largest error source for

The associate editor coordinating the review of this manuscript and approving it for publication was Giambattista Gruosso.

straightness measurement of the long workpiece profile [11]. Although the STP method of profile reconstruction doesn't have the zero-adjustment error and data processing error, this method has the following disadvantages. Firstly, the lateral resolution of the reconstructed profile is limited by the size of the probe. Secondly, quite a lot of scanning steps will have a longer scanning time. Although the sampling interval of the GTP method and the GTEP is not limited by the size of the probe. However, due to the distortion of higher harmonic components, this method has data processing error. In theory, the CTP method and the CTRP can obtain profile reconstruction without data processing error at a higher lateral resolution. But to adjust the relative position of multiple sets of reconstruction points, it is necessary to take a completely smooth known measurement profile. Therefore, it is difficult for these two methods to achieve high accuracy profile reconstruction and high lateral resolution in the meantime without data processing error.

In recent years, in addition to using the error separation method to eliminate the influence of the straightness of the guideway, there are also high-accuracy reference guideway and independent error measurement systems. Taylor Hobson achieves ultra-high straightness through the use of a high-accuracy reference guideway, with a straightness error of 80nm/200mm, and the measurement system accuracy is 0.15μm [12]. However, manufacturing ultra-high-accuracy reference guideways are expensive and time-consuming. A more widely used solution is online error compensation, which is achieved by designing an independent error measurement system. In the non-contact measurement of freeform optical surfaces with nanometer accuracy, LuphoScan and NANOMEFOS are two commercial Products [13], [14]. The LuphoScan 420 profiler has a range of 420 mm $\times$ 100 mm, and the system uncertainty is 50 nm (2σ). The measurement range of NANOMEFOS is φ500mm $\times$ 100mm, and the measurement uncertainty is 30 nm (2σ). However, designing an independent error measurement loop system usually requires a large number of high-accuracy sensors and is expensive, making the overall cost-prohibitive.

In recent studies, various methods have been continuously proposed to solve the problem of data processing error with high lateral resolution [15]–[18]. Zhai *et al.* used the interferometer as a multi-probe, developed a new translational rotation difference method to separate the straightness error, yaw error, and zero-adjustment error, and achieved profile reconstruction with high accuracy and high lateral resolution [19], [20]. The 4-probe and 6-probe measurement methods proposed by Chen *et al.* [21], [22] can eliminate the straightness error, zero-adjustment error, and yaw error. If the error of the probe itself is ignored, the exact profile reconstruction can be achieved with a higher lateral resolution. Clemens Elster *et al.* developed a new multi-probe method [23], [24], which uses coupled multiple distance sensors and an additional collimator to eliminate both scanning stage errors as well as systematic sensor offset errors. Eric H.K. Fung *et al.* proposed a new method using eight

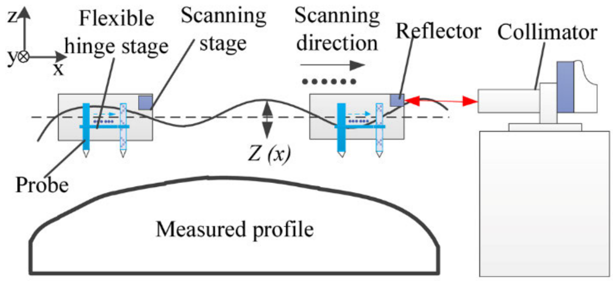

FIGURE 1. Structure of the measuring system.

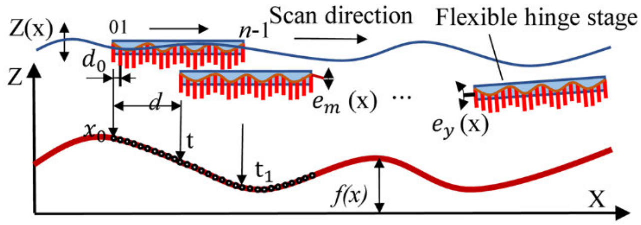

FIGURE 2. Schematic diagram of the scanning acquisition process.

probes to separate the straightness, yaw, and pitch error of the guideway [25]. For the profile measurement of freeform surfaces, since the motion error of six degrees of freedom per axis must be considered, error separation is still challenging. This means that very complex probe systems and related reconstruction algorithms are necessary, but the increase in complexity usually leads to an increase in the uncertainty of the measurement results [26].

To simplify the multi-probe system and improve reliability, obtain high measurement accuracy and lateral resolution. Since the flexure hinge stage has extra high repeatability [27], the probe positions can be detected with high accuracy in real-time. Therefore, in this paper, we propose a virtual multi-probe system and its corresponding new error separation method. The virtual multi-probe system is based on the flexible hinge and collimator. The collimator is used to detect the yaw error. By using the flexible hinge, a single probe can realize and expand the multi-probe scanning measurement function, which can separate the straightness error and the zero-adjustment error and can reconstruct the measured profile with high lateral resolution.

II. THE VIRTUAL MULTI-PROBE SCANNING MEASUREMENT SYSTEM

A. THE STRUCTURE OF THE MEASUREMENT SYSTEM

As shown in Fig. 1, the measurement system mainly includes a scanning stage, a flexible hinge stage, and a collimator. The flexible hinge stage includes a flexible hinge, a voice coil motor, an optical probe, and a linear encoder. The flexible hinge stage fixed on the scanning stage to move together along the scanning direction. The yaw error of the scanning stage is measured by the collimator.

The system realized the multi-probe function by a single probe that fixed on the flexible hinge stage. The flexible hinge stage has a millimeter-level travel range and driven

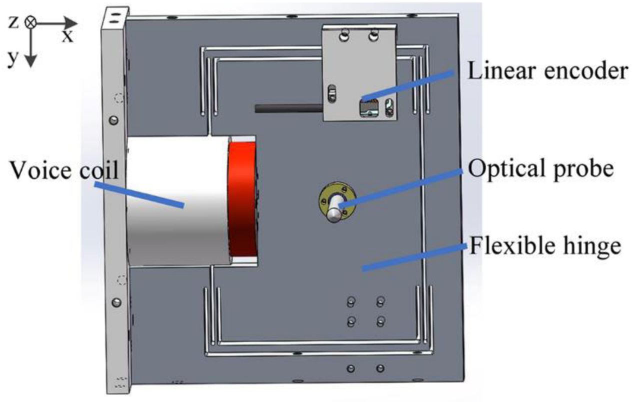

FIGURE 3. Schematic diagram of the flexible hinge stage.

by a voice coil motor to realize the function of multiple-probe. The measurement process of the virtual multi-probe scanning measurement system is shown in Fig. 1 and Fig. 2. The scanning stage moved with equal interval d, and the flexible hinge stage is sampled with equal interval d_0 in each shear point of the scanning stage. Among them, d is the shear length of the scanning stage, d_0 is the sampling interval of the flexible hinge stage, n is the number of sampling points of the flexible hinge stage each time, and it must be ensured that the length of each sampling profile of the flexible hinge stage is longer than d. The pitch angle of the scanning stage is detected by the collimator.

Repeat the above two steps until the scanning of the entire profile is completed, and the profile length of each scanning of the flexible hinge stage is $(n-1)\cdot d_0$. Due to the shear length of the scanning stage is $d < (n-1)\cdot d_0$, the two adjacent scans will have coincident sampling profiles. The profile interval $t - t_1$ of the two adjacent scans is the same profile, which should be equivalent in theory. According to the coincident point of the profile to eliminate the straightness error, zero-adjustment error, and reconstruct the profile.

B. DESIGN OF THE FLEXIBLE HINGE STAGE

The flexible hinge stage should have high accuracy and long stroke, the stroke is designed to be longer than 1 millimeter. To realize the long stroke of the stage, a flexible hinge structure with a multi-stage compound parallel blade bending is designed. The design results are shown in Fig. 3. The flexible hinge stage includes the flexible hinge, voice coil motor, optical probe, and linear encoder.

As shown in Fig. 4(a), an experimental device for detecting the straightness of the flexible hinge stage that uses a high precision plane with a flatness of 30nm to detect the straightness of the flexible hinge stage. To test the straightness of the flexible hinge stage at sampling positions, the flexible hinge moves 6 times in the position rang of $\pm 500\mu$m, and the probe samples 20 points each time. Fig. 4(b) is the straightness error of the flexible hinge stage after removing the linear trend of the optical probe value. The value of the six sets of data all in the range of [−30nm, 30nm]. Since the data itself contains

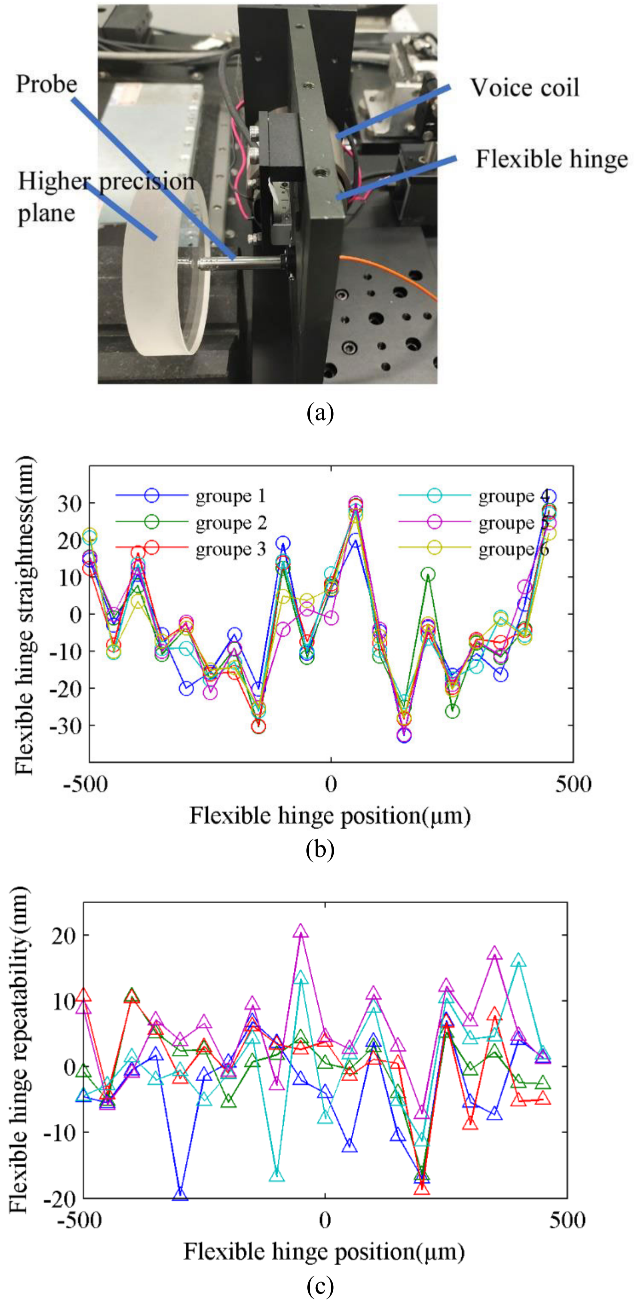

FIGURE 4. Straightness and repeatability of the flexible hinge stage: (a) the experimental device, (b) the straightness of the flexible hinge, (c) the repeatability of height differences.

probe noise, the high accuracy flat (within 1mm) surface shape error and the high precision plane profile error, the straightness of the flexible hinge itself is better than ±30nm

As shown in Fig. 4(a), to measure the repeatability of the flexible hinge stage at sampling positions, the flexible hinge moves 6 times in the position rang of $\pm 500\mu$m, and the probe samples 20 points each time. As shown in Fig. 4(c), the maximum probe deviation value of the 6 times is approximately 20nm, which close to the repeatability accuracy level of the probe itself. So, it is obvious that the flexible hinge stage has extra high repeatability.

C. THE ELIMINATION OF STRAIGHTNESS, ZERO-ADJUSTMENT ERROR

As shown in Fig. 2, the sampling interval of the flexible hinge stage is d_0, the scanning movement of the scanning stage is d, the probe output is m(i, x) $(i = 0, 1, 2, \ldots, N)$, i is scanning stage sampling points. Define the measured profile of the workpiece as $f(x)$, the straightness error of the scanning stage as $Z(x)$, the pitch angle of the scanning stage as $\propto_i$, and the straightness of the flexible hinge stage as $e_m(j)$ $(j = 0, 1, 2, \ldots, n\text{-}1)$, n is the number of sampling points of the flexible hinge stage each time, and $\propto_i$ is measured by the collimator.

Define the starting point of sampling as x_0, then the output equation of the probe during the first acquisition:

$$m(0, x_0 + jd_0) = Z(x_0) + f(x_0 + jd_0) + e_m(j) + jd_0 sin(\propto_0) + C \tag{1}$$

The output of the probe during the second acquisition:

$$m(1, x_0 + d + jd_0) = Z(x_0 + d) + f(x_0 + d + jd_0) + e_m(j) + jd_0 sin(\propto_1) + C \tag{2}$$

Define $x_N = x_0 + Nd, x_{N-1} = x_0 + (N-1)d$.Similarly, The output of the probe during the N+1th acquisition:

$$m(N, x_N + jd_0) = Z(x_N) + f(x_N + jd_0) + e_m(j) + jd_0 sin(\propto_N) + C \tag{3}$$

As shown in Fig. 2, since $t - t_1$ samples the same profile, it should be equal in theory, namely in (1) and (2):

$$f(x_0 + jd_0) = f\left(x_0 + d + \left(j - \frac{d}{d_0}\right)d_0\right), \quad \frac{d}{d_0} \le j \le n-1 \tag{4}$$

Simultaneous equations (1), (2), and (4), we can get:

$$Z(x_0 + d) - Z(x_0) = m\left(1, x_0 + d + (j - \frac{d}{d_0})d_0\right) - m(0, x_0 + jd_0) - (j - \frac{d}{d_0})d_0 sin(\propto_1) + jd_0 sin(\propto_0) - e_m(j - \frac{d}{d_0}) + e_m(j) \tag{5}$$

Similarly, the difference equation of the straightness during the third acquisition is:

$$Z(x_0 + 2d) - Z(x_0 + d) = m\left(2, x_0 + 2d + (j - \frac{d}{d_0})d_0\right) - m(1, x_0 + d + jd_0) - (j - \frac{d}{d_0})d_0 sin(\propto_2) + jd_0 sin(\propto_1) - e_m\left(j - \frac{d}{d_0}\right) + e_m(j) \tag{6}$$

Similarly, the difference equation of the straightness during the N+*1*th acquisition is:

$$Z(x_N) - Z(x_{N-1}) = m\left(N, x_N + (j - \frac{d}{d_0})d_0\right) - m(N-1, x_{N-1} + jd_0) - (j - \frac{d}{d_0})d_0 sin(\propto_N) + jd_0 sin(\propto_{N-1}) - e_m(j - \frac{d}{d_0}) + e_m(j) \tag{7}$$

The cumulative summation of the straightness difference equations yields:

$$Z(x_N) - Z(x_0) = \sum_{i=0}^{N}[m\left(i+1, x_0 + (i+1)d + (j - \frac{d}{d_0})d_0\right) - m(i, x_0 + id + jd_0) - (j - \frac{d}{d_0})d_0 sin(\propto_{i+1}) + jd_0 \sin(\propto_i)] + (N+1)\left(e_m(j) - e_m\left(j - \frac{d}{d_0}\right)\right) \tag{8}$$

Define $Z(x_0) = 0$, (8) can eliminate the influence of the straightness error of the flexible hinge stage after removing the linear trend, and the straightness of the scanning stage can be obtained.

$$Z(x_N) = \sum_{i=0}^{N}[m\left(i+1, x_0 + (i+1)d + (j - \frac{d}{d_0})d_0\right) - m(i, x_0 + id + jd_0) - (j - \frac{d}{d_0})d_0 sin(\propto_{i+1}) + jd_0 \sin(\propto_i)], \quad \frac{d}{d_0} \le j \le n-1 \tag{9}$$

From (9), $(n - d/d_0)$ sets of straightness error $(Z(x_N))$ of the scanning stage can be obtained, and the average of multiple sets of data can suppress the influence of the noise, and the measurement result is more reliable.

D. THE RECONSTRUCTION OF THE PROFILE

Define $Z(x_0) = 0$, summing up and averaging the multiple sets of straightness of (8):

$$Z(x_N) = \frac{1}{n - \frac{d}{d_0}} \times \sum_{j=\frac{d}{d_0}}^{n-1} \sum_{i=0}^{N} [m\left(i+1, x_0 + (i+1)d + (j - \frac{d}{d_0})d_0\right) - m(i, x_0 + id + jd_0) - (j - \frac{d}{d_0})d_0 \sin(\propto_{i+1})$$

$$+jd_0\sin(\propto_i)] + \frac{N+1}{n-\frac{d}{d_0}}\sum_{j=\frac{d}{d_0}}^{n-1}\left[e_m(j-\frac{d}{d_0}) - e_m(j)\right] \quad (10)$$

Define $\frac{N+1}{n-\frac{d}{d_0}}\sum_{j=\frac{d}{d_0}}^{n-1}\left[e_m(j-\frac{d}{d_0}) - e_m(j)\right] = C_1$, then:

$$\begin{aligned}Z(x_N) = &\frac{1}{n-\frac{d}{d_0}} \times \sum_{j=\frac{d}{d_0}}^{n-1}\sum_{i=0}^{N}\\ &[m\left(i+1, x_0+(i+1)d+(j-\frac{d}{d_0})d_0\right)\\ &-m(i, x_0+id+jd_0)\\ &-(j-\frac{d}{d_0})d_0\sin(\propto_{i+1})\\ &+jd_0\sin(\propto_i)] + C_1\end{aligned} \quad (11)$$

According to (11), after removing the linear trend in (11), we can obtain the $Z(x_N)$ that not have the C_1.Then the output of the $N+1$th acquisition of the probe is:

$$\begin{aligned}m\left(N, x_N+(j-\frac{d}{d_0})d_0\right) = f&\left(x_N+(j-\frac{d}{d_0})d_0\right)\\ &+Z(x_N)\\ &+\left(j-\frac{d}{d_0}\right)d_0\sin(\propto_N)\\ &+e_m\left(j-\frac{d}{d_0}\right)+C\end{aligned} \quad (12)$$

After removing the linear trend in (12), we can obtain the reconstructed profile $f(\mathrm{x})$:

$$\begin{aligned}f\left(x_N+(j-\frac{d}{d_0})d_0\right) = m&\left(N, x_N+(j-\frac{d}{d_0})d_0\right)\\ &-Z(x_N)-(j-\frac{d}{d_0})d_0 sin(\propto_N)\\ &-e_m(j-\frac{d}{d_0})\end{aligned} \quad (13)$$

In (13), the reconstructed profile contains only the error $e_m(x)$, but this error does not accumulate as the measurement length increases. Since the designed flexible hinge stage straightness error range is within ±30nm, compared with the sub-micron accuracy the influence can be ignored.

III. SIMULATION

To prove and verify the new virtual multi-probe scanning system and the method proposed in this paper, and to study the reconstruction accuracy of the virtual multi-probe measuring system under the main error influencing factors. An aspheric profile is adopted as the simulation and measurement profile, the equation expression is:

$$Z = br + \frac{cr^2}{1+\sqrt{1-\left(1-(1+k)\times c^2r^2\right)}} \quad (14)$$

In(14), r is the radial coordinates of aspheric surface, b is the tilt of the asphere, Z is the sagittal height of the asphere, c is the curvature of vertex, and k is the conic constant. The values of parameters b, c, and k are 0, −0.00004, −0.4 respectively. The aspheric surface length is 100 mm. Define the sampling interval (d) of the scanning stage as 0.5 mm, so the number of steps $N+1$ is 201, the sampling interval of the flexible hinge stage (d_0) as 50μm, and the number of sampling points n of the flexible hinge stage as 20. As shown in Fig. 5, it is the simulated aspheric profile.

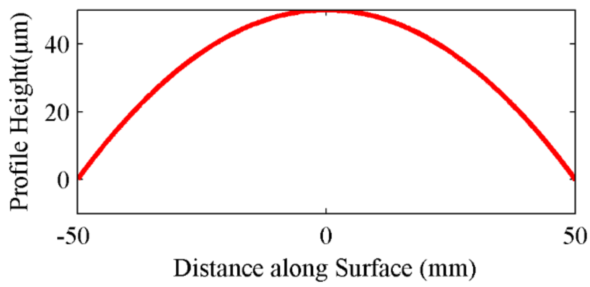

FIGURE 5. Simulated aspheric profile.

Although the proposed new method can reconstruct the surface profile accurately in theory. Due to the installation error, position error, vibration and probe noise and other errors in the actual system, we selected the non-parallel error of the scanning stage and the flexible hinge stage, the position error of the scanning stage and the flexible hinge stage, the straightness error of the flexible hinge stage, the probe noise and vibration, the collimator error as the main error factor to study the influence.

As shown in Fig. 6(a), the installation non-parallel error is set to 0.1°; As shown in Fig. 6(b), the straightness error of the flexible hinge stage amplitude is set to ±30nm random error. As shown in Fig. 6(c), the yaw error is set according to the collimator accuracy, and its amplitude is set to ±2.5μrad random error; As shown in Fig. 6(d), the position error is set according to the accuracy of the linear encoder, the position error of the scanning stage is set to ±0.5μm, and the flexible hinge stage amplitude is set to ±0.1μm random error; The environmental vibration value is measured by experiment, the probe noise is set according to its accuracy, and the vibration and probe noise amplitude is set to ±10nm random error.

Simulation step, step 1, the theoretical horizontal x coordinate of the sampling point of the profile is $(x_0+id+jd_0)$ position, the position of the scanning stage plus the amplitude ±0.5μm random position error s_1, $r1$ is a random number in the range of [0,1]. Due to the non-parallel error caused by the installation, the position of the scanning stage must be multiplied by $cos\theta$; The displacement of the flexible hinge stage plus the random position error s_2 of amplitude ±0.1μm, $r2$ is a random number in the range [0,1].

$$s_1[201, 1] = r1[201, 1]-0.5 \quad (15)$$

$$s_2[1, 20] = r2[1, 20]\cdot 0.2 - 0.1 \quad (16)$$

Then, the actual horizontal x coordinate of the sampling point of the measured profile is:

$$x_a = x_0 + (id + s_1[i+1, 1]) * cos\theta + jd_0 + s_2[1, j] \quad (17)$$

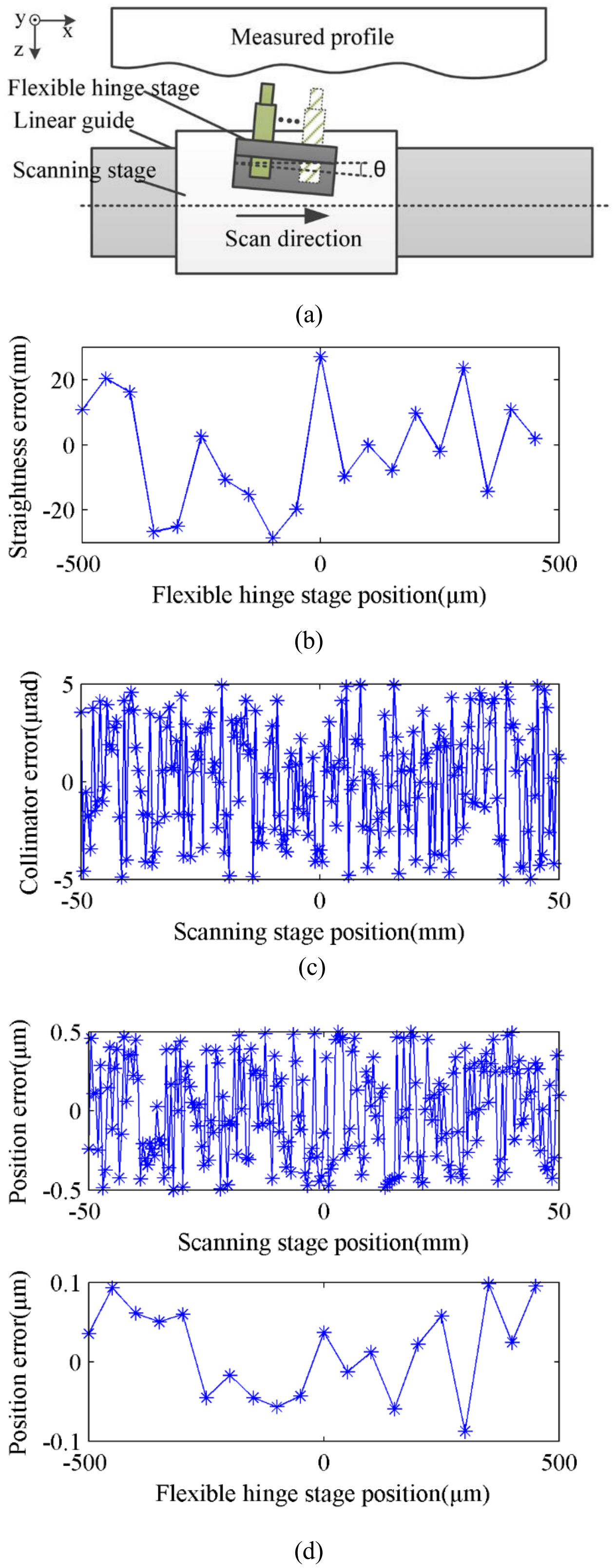

FIGURE 6. The main error of the measurement system:(a) the installation error, (b) the straightness of the flexible hinge, (c) the collimator error, (d) the position error of the scanning stage, and the flexible hinge stage.

Then, the profile at the actual sampling point is:

$$m(i, x_a) = f(x_a) + Z(x_0 + id) + jd_0 sin(\propto_i) \quad (18)$$

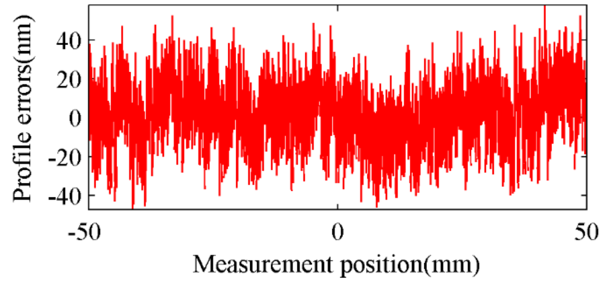

FIGURE 7. Profile reconstruction simulation errors.

Step 2, the output of the probe plus the noise random error h of amplitude $\pm 0.01\mu$m. Then, add the zero-adjustment error (e_m) of the probe at each position on the flexible hinge stage. The zero-adjustment error is a randomly assigned amplitude of $\pm 0.03\mu$ m. Due to the extremely high repeatability of the flexible hinge stage, the zero-adjustment error will remain unchanged after distribution, and the probe output at this time is:

$$m(i, x_a) = f(x_a) + Z(x_0 + id) + jd_0 sin(\propto_i) + h[i, j] + e_m[j] \quad (19)$$

Step 3: The output value of the probe plus the random error ($\propto_e$) of the amplitude of the collimator is $\pm 2.5\mu$rad. The probe output at this time is:

$$m(i, x_a) = f(x_a) + Z(x_0 + id) + jd_0 sin(\propto_i + \propto_e[i]) + h[i, j] + e_m[j] \quad (20)$$

Step 4: Use the coincidence point profile to eliminate the straightness error and zero-adjustment error.

Step 5. The reconstruction of the profile

As shown in Fig. 7, under the condition of adding the above error factors, the simulation error PV and RMS of the profile reconstruction are 0.09μm and 0.014μm, respectively. Without the influence of error, the profile reconstruction error is 6×10^{-12}nm, and the error is the calculation error caused by the number of decimal points reserved by software.

IV. EXPERIMENT

The following experiment is conducted to verify the new method. As shown in Fig. 8, we developed the virtual multi-probe scanning measurement system. The measured surface is the aspherical surface described in (14), and the flexible hinge stage is fixed on the air-floating linear motion scanning stage. The collimator measures the pitch angle of the scanning stage in real-time. The measured workpiece length is 100 mm, the sampling interval(d) of the scanning stage is 0.5 mm, so the number of steps $N + 1$ is 201, the sampling interval of the flexible hinge stage (d_0) is 50μm, and the number of sampling points n of the flexible hinge stage is 20.

Fig. 9 shows the profile error measured by scanning directly with a single optical probe without straightness error separation. Due to the straightness error of the scanning stage, the profile errors of the measured surface: 0.58μm (PV),0.12μm (RMS), and 0.09 μm (Ra).

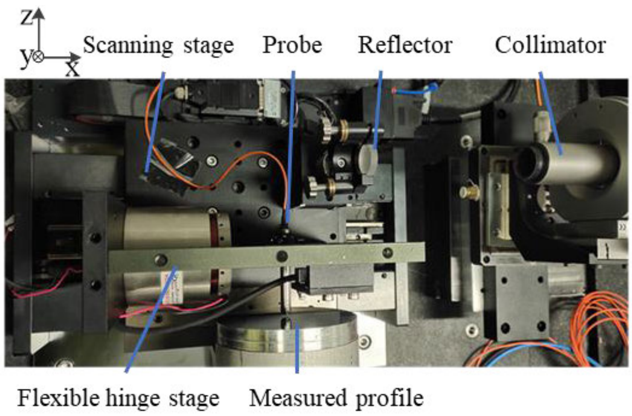

FIGURE 8. Experimental device.

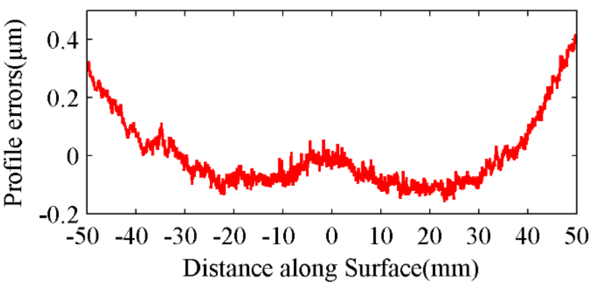

FIGURE 9. Profile errors measured by single probe direct scanning.

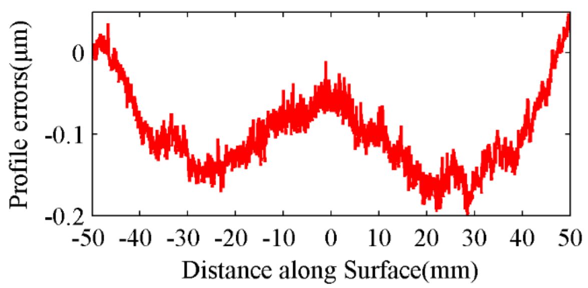

FIGURE 10. The profile reconstruction errors of the new method.

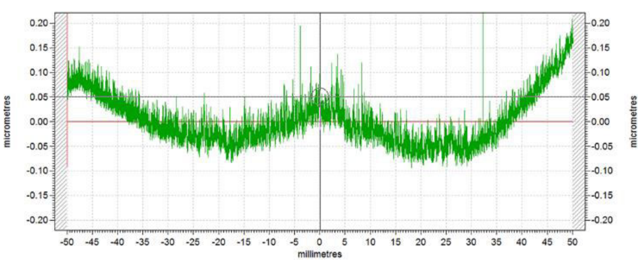

FIGURE 11. The profile reconstruction error of the Taylor PGI 1240 profilometer.

Fig. 10 shows the measured results from the new method. As shown in Fig. 10, the profile errors measured by the new method are 0.25μm (PV), 0.04 μm (Ra), and 0.11μm (RMS). Fig. 11 shows the profile errors measured by the Taylor Hobson PGI1240 profilometer. The profile errors measured by the PGI1240 are 0.33 μm (PV), 0.04μm (Ra). Fig. 12 shows the profile error comparison between the new method and

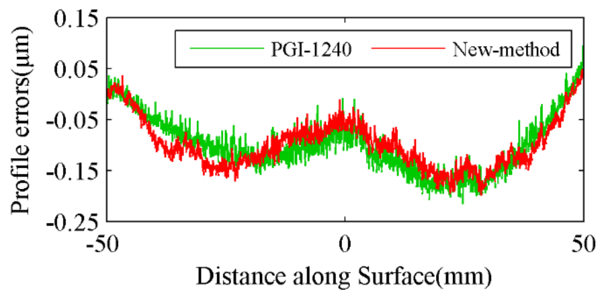

FIGURE 12. The profile reconstruction errors of different methods (the new method, and the PGI 1240).

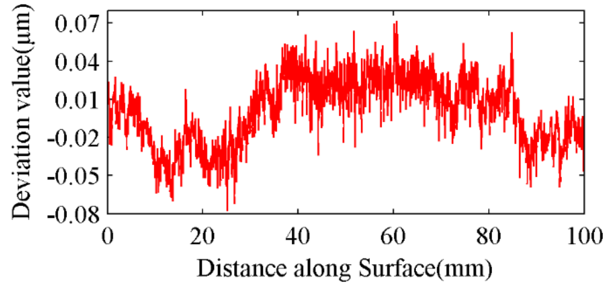

FIGURE 13. The deviation between the two methods (the new method, and the PGI1240).

the PGI1240 that the profile measured results after leveling. Fig. 13 shows the profile error deviation between the new method and PGI1240 after leveling. From Fig. 12 and Fig. 13, we can find that the results measured by the new method have a very high consistency with the PGI1240 profiler, and the deviation value is less than 0.08μm, which may be due to the use of different probes (contact and non-contact) or caused by installation errors during two measurements.

V. CONCLUSION

The new method proposed in this paper uses a single probe to realize and expand the multi-probe scanning measurement function through the flexible hinge stage. The exact reconstruction of the profile with high lateral resolution can be achieved under the conditions of zero-adjustment error, straightness error, and yaw error. In theory, the straightness error of the scanning stage can be completely separated, and the cumulative amplification effect of zero-adjustment error of the flexible hinge stage can be eliminated by this algorithm. This new method has the advantages of the general multi-probe method, and can also avoid various problems in the existing measurement methods. The feasibility of the new method is verified through theoretical analysis, simulation, and experiment. Compared with the commercial PGI1240 profilometer, the measurement deviation of the proposed virtual multi-probe scanning measurement system is less than 0.08μm@100mm.

REFERENCES

[1] W. T. Estler, "Calibration and use of optical straightedges in the metrology of precision machines," *Opt. Eng.*, vol. 24, no. 3, pp. 372–379, Jun. 1985.

[2] A. Campbell, "Measurement of lathe Z-slide straightness and parallelism using a flat land," *Precis. Eng.*, vol. 17, no. 3, pp. 207–210, Jul. 1995.
[3] C. J. Evans, R. J. Hocken, and W. T. Estler, "Self-calibration: Reversal, redundancy, error separation, and absolute testing,'" *CIRP Ann.*, vol. 45, no. 2, pp. 617–634, 1996.
[4] H. Tanaka, K. Tozawa, H. Sato, M. O-Hori, H. Sekiguchi, and N. Taniguchi, "Application of a new straightness measurement method to large machine tool," *CIRP Ann.*, vol. 30, no. 1, pp. 455–459, Jan. 1981.
[5] K. Tozawa, H. Sato, and M. O-Hori, "A new method for the measurement of the straightness of machine tools and machined work," *J. Mech. Des.*, vol. 104, no. 3, pp. 587–592, Jul. 1982.
[6] H. Tanaka and H. Sato, "Extensive analysis and development of straightness measurement by sequential-two-points method," *J. Eng. Ind.*, vol. 108, no. 3, pp. 176–182, Aug. 1986.
[7] S. Kiyono and W. Gao, "Profile measurement of machined surface with a new differential method," *Precis. Eng.*, vol. 16, no. 3, pp. 212–218, Jul. 1994.
[8] W. Gao and S. Kiyono, "High accuracy profile measurement of a machined surface by the combined method," *Measurement*, vol. 19, no. 1, pp. 55–64, Sep. 1996.
[9] K. Kounosu and T. Kishi, "Measurement of surface profile using smoothed serial three point method," *J. Jpn. Soc. Precis. Eng.*, vol. 61, no. 5, pp. 641–645, 1995.
[10] W. Gao and S. Kiyono, "On-machine profile measurement of machined surface using the combined three-point method," *JSME Int. J. C*, vol. 40, no. 2, pp. 253–259, 1997.
[11] W. Gao, J. Yokoyama, H. Kojima, and S. Kiyono, "Precision measurement of cylinder straightness using a scanning multi-probe system," *Precis. Eng.*, vol. 26, no. 3, pp. 279–288, Jul. 2002.
[12] *Form Talysurf PGI*, AMETEK Inc., Leicester, U.K., 2016. [Online]. Available: https://FTS-PGI-Series_Spec_LowRes_CHN-Form
[13] C. W. Weg, G. Berger, T. May, R. Nicolaus, and J. Petter, "Method and device for measuring surfaces in a highly precise manner," U.S. Patent 8 736 850 B2, May 27, 2014.
[14] R. Henselmans, L. A. Cacace, G. F. Y. Kramer, P. C. J. N. Rosielle, and M. Steinbuch, "The NANOMEFOS non-contact measurement machine for freeform optics," *Precis. Eng.*, vol. 35, no. 4, pp. 607–624, Oct. 2011.
[15] Z.-Q. Yin and S.-Y. Li, "Exact straightness reconstruction for on-machine measuring precision workpiece," *Precis. Eng.*, vol. 29, no. 4, pp. 456–466, Oct. 2005.
[16] Z.-Q. Yin and S.-Y. Li, "High accuracy error separation technique for on-machine measuring straightness," *Precis. Eng.*, vol. 30, no. 2, pp. 192–200, Apr. 2006.
[17] Z.-Q. Yin, "Exact wavefront recovery with tilt from lateral shear interferograms," *Appl. Opt.*, vol. 48, no. 14, pp. 2760–2766, 2009.
[18] Z. Yin, S. Li, and F. Tian, "Exact reconstruction method for on-machine measurement of profile," *Precis. Eng.*, vol. 38, no. 4, pp. 969–978, Oct. 2014.
[19] D. Zhai, S. Chen, X. Peng, and G. Tie, "Absolute profile test by multi-sensor scanning system with relative angle measurement," *Meas. Sci. Technol.*, vol. 29, no. 11, Nov. 2018, Art. no. 115205.
[20] D. Zhai, S. Chen, X. Peng, and G. Tie, "Absolute flat test using rotated and multi-shifted maps with relative tilt measurement," *Opt. Lasers Eng.*, vol. 114, pp. 121–128, Mar. 2019.
[21] X. Chen, C. Sun, L. Fu, and C. Liu, "A novel reconstruction method for on-machine measurement of parallel profiles with a four-probe scanning system," *Precis. Eng.*, vol. 59, pp. 224–233, Sep. 2019.
[22] X. Chen, C. Sun, L. Fu, and C. Liu, "A novel six-probe method for the measurement and exact reconstruction of a pair of parallel profiles," *IEEE Access*, vol. 8, pp. 68158–68168, 2020.
[23] C. Elster, I. Weingärtner, and M. Schulz, "Coupled distance sensor systems for high-accuracy topography measurement: Accounting for scanning stage and systematic sensor errors," *Precis. Eng.*, vol. 30, no. 1, pp. 32–38, Jan. 2006.
[24] M. Schulz, "Traceable multiple sensor system for measuring curved surface profiles with high accuracy and high lateral resolution," *Opt. Eng.*, vol. 45, no. 6, Jun. 2006, Art. no. 060503.
[25] E. H. K. Fung, M. Zhu, X. Z. Zhang, and W. O. Wong, "A novel Fourier-eight-sensor (F8S) method for separating straightness, yawing and rolling motion errors of a linear slide," *Measurement*, vol. 47, pp. 777–788, Jan. 2014.
[26] S. Chen, S. Xue, and D. Zhai, "Measurement of freeform optical surfaces: Trade-off between accuracy and dynamic range," *Laser Photon. Rev.*, vol. 14, no. 5, pp. 1–32, May 2020.
[27] A. H. Slocum, "8.6 flexural bearings of chapter 8," in *Precision Machine Design*. Upper Saddle River, NJ, USA: Prentice-Hall, 1992, pp. 521–538.

NING CHAI received the M.S. degree in mechanical engineering from the Guangdong University of Technology, in 2017, where he is currently pursuing the Ph.D. degree in mechanical engineering with the State Key Laboratory of Precision Electronic Manufacturing Technology and Equipment. His current research interests include optical measurement technology and flexible hinge stage technology.

ZIQIANG YIN received the M.S. and Ph.D. degrees in mechatronic engineering from the National University of Defense Technology, in 1996 and 2003, respectively. He is currently a Professor with the State Key Laboratory of Precision Electronic Manufacturing Technology and Equipment, Guangdong University of Technology. His research interests include optical measurement technology, ultra-precision machine tool and component design, and ultra-precision cutting, grinding, and polishing processing.

JIANHUA YAO received the B.S. degree from the School of Mechanical Engineering, Wuhan Polytechnic University, in 2015. He is currently pursuing the Ph.D. degree in mechanical engineering with the State Key Laboratory of Precision Electronic Manufacturing Technology and Equipment, Guangdong University of Technology. His current research interests include aerostatic bearing technology and high-precision equipment.